DOI: 10.21062/mft.2022.021 http://www.journalmt.com

The Mechanical Analysis of ELM Joint under Coupling Field

Xianewei Wang (0000-0001-9804-0403)[1], Xiuxiang Chen (0000-0002-5484-3228)[1], Peng Han (0000-0002-3892-7499)[2], Qinxian Jiang (0000-0001-9682-2196)[1], Xiulian Li (0000-0001-9441-261X)[1]
[1]Jiangsu University of Technology, Changzhou 213001, China. E-mail: wangxw@jsut.edu.cn, 582763914@qq.com, qqaa611@163.com, 936303415@qq.com
[2]SANY Heavy Industry Co.,Ltd, Huzhou, 313000, China. E-mail: hanp86@qq.com

The Edge Localized Mode coil is the key component to prohibit the phenomena of disruptive instability occurring in the edge of Tokamak plasma. The coil is made of Stainless Steel Jacketed Mineral Insulated Conductors. And the different pieces of conductor are connected by joints. During the normal operation of Tokamak device, the joints will be shocked by the electromagnetic and thermal loads. Thus, it is necessary to perform the mechanical analysis to verify whether or not the ELM joint has sufficient safety margin to resist the impact of the coupling field. To get the load boundary conditions for the mechanical analysis, the electromagnetic and thermal analysis are launched first. Then the obtained temperature and electromagnetic force density are inserted into the mechanical analysis model. And the equivalent stress is calculated subsequently. The analysis results indicate there is stress intensity. To mitigate the stress intensity, the local structural optimization is employed. Finally, the stress evaluation is carried out based on analytical design. The assessment results demonstrate the optimized model has sufficient safety margin to withstand the shock of multiple loads.

Keywords: ELM joint, Electromagnetic force, thermal load, Stress evaluation

1 Introduction

The quasi-periodic relaxation of transport barrier will be formed during the low mode to high mode transition, which will lead to a disruptive instability occurring in the edge region of Tokamak plasma, namely Edge Localized Mode (ELM) [1-3]. To suppress the phenomena of ELM, nine sets of coil with the shape of picture frame are designed and arranged in the toroidal direction of vacuum vessel. Each set of ELM coil is comprised of the upper, equatorial and lower coils positioned in the poloidal direction. The operating environment of ELM coil is severe in terms of strong radiation and high temperature, which precludes the use of organic insulating materials. The feasible mineral insulation is compacted Magnesium Oxide (MgO) powder, which is housed by Inconel 625. To guarantee adequate lifetime, the Copper-Chromium-Zirconium (CuCrZr) alloy is used as conductor to carry the large current. Thus, the final ELM coil is the Stainless Steel Jacketed Mineral Insulated Conductors (SSMIC) [4-7]. The inner diameter of CuCrZr is of 33.3 mm. The thickness of CuCrZr, MgO and Inconel 625 are 6.35 mm, 2.5 mm and 4 mm respectively. The ELM coil is winded by several pieces to form six turns. The different pieces of conductor are connected by joints. The joints are classified into two different types based on the shapes, namely the straight and arc joints as shown in Fig. 1.

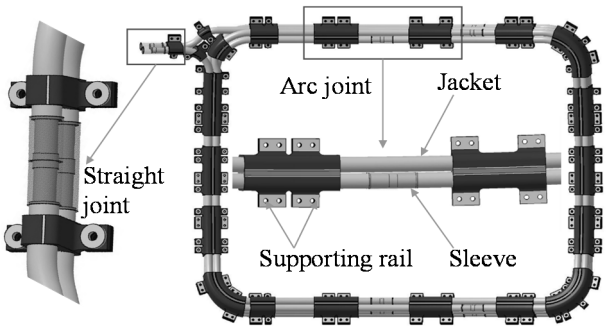

Fig. 1 *The ELM joints*

The straight joints are used to connect the coil body and feeders. The arc joints are used to form the six turns of coil body. And we mainly focus on the arc joint in the paper. In the joint region, the two different pieces of conductor are packed by a 200 mm-long Inconel 625 sleeve with the thickness of 3 mm. The two ends of the sleeve are welded with the jacket. The thickness of the impacted MgO in the joint region is 6.5 mm. The butt brazing scheme is selected to connect the inner CuCrZr joint. Before the brazing, a 1 mm-thick and 10 mm-long copper ring is installed at the interface to improve the brazing performance [8]. The design lifetime of joint is twenty years without maintenance during the period. Thus, the requisite reliability of joint is needed under multi load cases during normal operation. The loads that ELM joints need to bear are mainly the electromagnetic force and the thermal loads. The thermal loads include the Joule

heat and plasma irradiation. In the paper the electromagnetic force will be calculated first. Then, the temperature caused by Joule heat and plasma radiation is analysed subsequently. Finally, the obtained electromagnetic force density and temperature field is applied as boundary condition to perform the mechanical analysis.

2 The loads calculation for ELM joint

2.1 The electromagnetic force calculation

The electromagnetic (EM) force will be induced due to the interaction of ELM coil current and background magnetic field derived from the device magnet system and plasma current. The plasma current varies with the operation stage. The magnetic field reaches peak value at the scenario of End of Burn (EOB). Thus, it is chosen to carry out the electromagnetic analyses. The magnetic field is calculated based on the method of Magnetic Vector Potential (MVP) by using the software ANSYS Maxwell. The plasma current and background field coils are simulated by current source [9] in the equivalent calculation model shown in Fig. 2, which is helpful to simplify the analysis model. The simulation result of magnetic field is presented in Fig. 3. The maximum magnetic field of upper, equatorial and lower ELM coils are 4.67 T, 4.84 T and 4.64 T respectively. Thus, the joint of equatorial ELM coil is selected conservatively to carry out the following mechanical analysis.

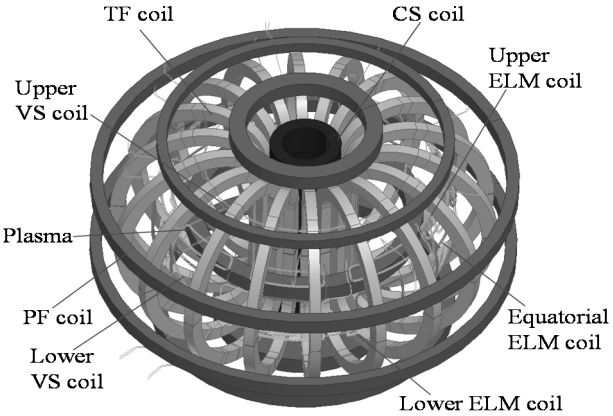

Fig. 2 *The equivalent magnetic calculation model for in vessel coil*

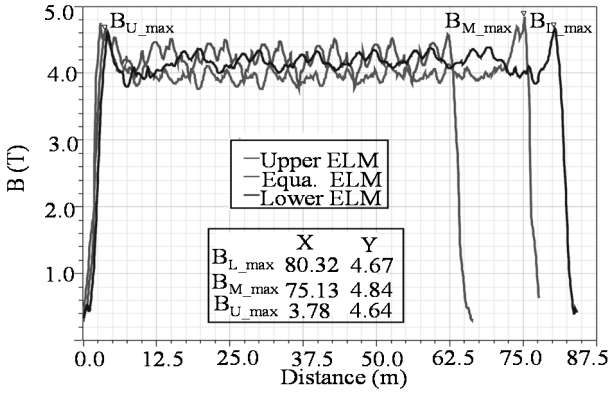

Fig. 3 *The magnetic field of ELM coil*

Once the magnetic field at the joint has been calculated. The electromagnetic force could be calculated based on Ampere's law. The current flowing through ELM conductor is 15 kA per turn. Assuming the current direction is anti-clockwise. The average magnetic density on the joint is 4 T. Thus, the corresponding electromagnetic force density is about 60 KN·m^{-1}. And the direction of Lorentz force is perpendicular to vacuum vessel wall as shown in Fig. 5. Where B_T represents the toroidal magnetic field. Cause it is parallel with the current, it will not generate electromagnetic force on the joint. B_P is the poloidal magnetic field. Since it is perpendicular to the current direction, it is the main magnetic field that induce the large electromagnetic force. The length of every joint conductor is 1.135 m. Therefore, the corresponding electromagnetic force on the inner CuCrZr copper conductor is 68.1 KN.

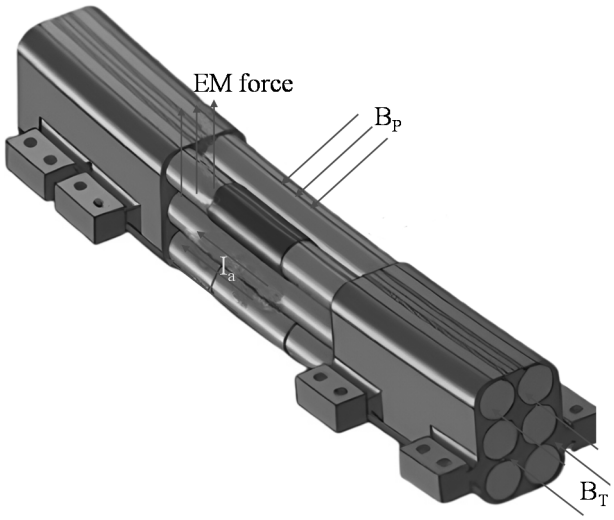

Fig. 4 *The direction of electromagnetic force on the equatorial ELM joint*

2.2 The thermal loads calculation

The thermal loads that ELM coil needs to bear are Joule heat and nuclear heat. The peak current flowing through ELM coil is 90 kA. The electrical resistivity of ELM conductor is 2.71 μΩ·cm. Then the Joule heat could be calculated based on the formula listed in equation (1). The calculated Joule heat density of ELM joint is 2.95 MW·m^{-3}. Concerning the nuclear heat, its distribution is approximately constant in the toroidal direction. While the nuclear heat attenuates exponentially in the direction perpendicular to the vacuum vessel wall. And the attenuation eigenvalue is about 0.14 m. Then the nuclear heat arrived at joint region could be calculated according to the formula presented in equation (2). The calculation result indicates the peak nuclear heat occurs at the top surface of clamp facing the plasma. Then it decreases gradually along the height direction of clamp. For the six-piece conductors, the nuclear heat distribution is different with position. The nuclear heat is relatively higher for the

outer exposed conductor. While the conductors at the two ends wrapped by clamps are hardly affected by plasma irradiation. Thus, the nuclear heat is smaller. The detailed distribution of nuclear heat is shown in Fig. 5.

$$q_1 = \frac{r I^2}{A^2} \text{ [W·m}^{-3}\text{]}, \quad (1)$$

$$q_2 = 2.5' \ e^{-r/0.14} \text{ [MW·m}^{-3}\text{]}, \quad (2)$$

Where:

r …Electrical resistivity of CuCrZr conductor at 100°C [μΩ·m],

I …Peak current flowing through the CuCrZr conductor [A],

A …Cross-sectional area of CuCrZr conductor [m²],

q_1 …Joule heat on the ELM joint [W·m⁻³],

q_2 …Nuclear heat on the ELM joint surface [MW·m⁻³],

r …Distance along the radial direction [m].

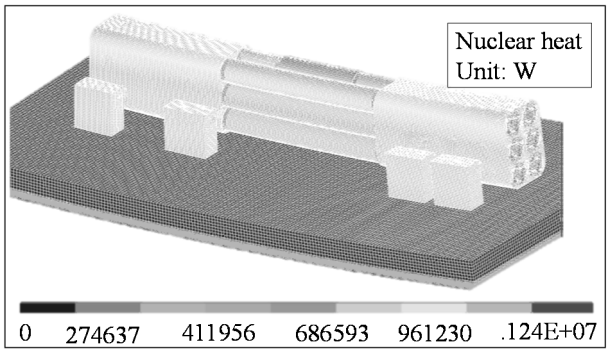

Fig. 5 *The distribution of nuclear heat on the equatorial ELM joint*

2.3 The temperature calculation of ELM joint

To avoid overheating, the ELM coil is cooled by water with inlet temperature of 100℃. The water velocity and convective heat transfer coefficient are 8 m·s⁻¹ and 34820 W·(m²·K)⁻¹ respectively. The convective heat flux is calculated based on Newton-cooling equation [10]. The detailed fluid-solid coupling analysis of coolant water and CuCrZr inner surface could be referenced from the references [11-12]. For the convenience of temperature calculation, the nuclear heat and Joule heat are treated as inner heat source. Then the thermal analysis degenerates to heat conduction. And the temperature could be could be calculated based on equation (3). The detailed temperature is calculated by ANSYS. The finite element model is shown in Fig. 6. The nuclear and joule heat are inserted as inner heat source. The temperature distribution is obtained by thermal solution. The highest temperature of CuCrZr conductor is 101.17℃. The temperature distribution of jacket and supporting rail are presented in Fig. 7 and Fig. 8. respectively.

$$\frac{\partial^2 T}{\partial x^2} + \frac{\partial^2 T}{\partial y^2} + \frac{\partial^2 T}{\partial z^2} + \Phi = 0 \,, \quad (3)$$

Where:

T …Temperature of ELM joint [℃],

x, y, z …Three components under Cartisan coordinate system [m],

Φ …Inner heat source [MW·m⁻³].

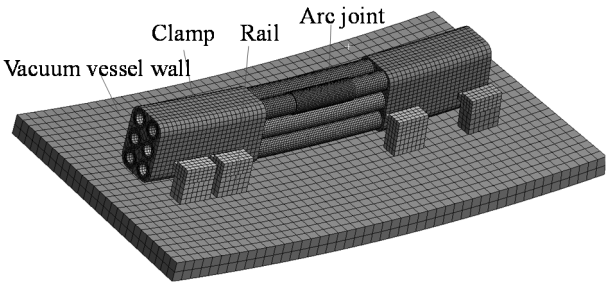

Fig. 6 *The finite element model of ELM joint*

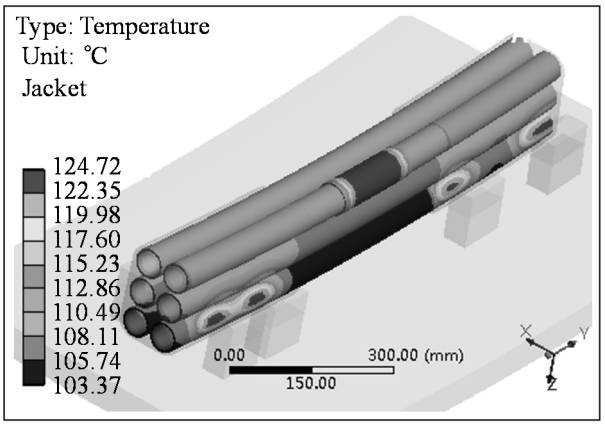

Fig. 7 *The temperature distribution on the jacket*

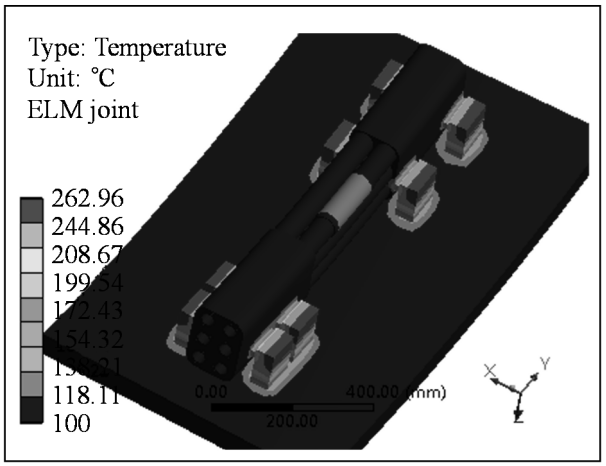

Fig. 8 *The temperature distribution on the ELM joint*

3 The thermal-electromagnetic-structural coupling analysis and structural optimization

3.1 The coupling field analysis

To verify the reliability of ELM joint under multi-load cases, the mechanical analysis is launched. The finite element model is the same as Fig. 6. But a few simplifications were made. For instance, the thread

connection components were excluded and the fillets of rails were ignored [13]. For the sake of distributing Lorentz force conveniently, the methods of sweeping, area mapping, multi-zone and size controlling are adopted to mesh the solid model. The sum number of element and node are 113300 and 2135000 respectively. The contact interfaces between components are simulated by using the element type of CONTACT 174. And bonded contact is imposed on these interfaces. The symmetric boundary condition is applied at the joint two ends. And the rails are bonded to the inner vacuum vessel wall. The outer vacuum vessel wall is fixed. The temperature field is imposed by reading into it from the thermal analysis result file. The electromagnetic force is applied on the node in the form of volumetric force. Finally, the equivalent stress is extracted through executing the solution module. The detailed stress distribution is presented in Fig. 9, 10 and 11. The maximum equivalent stress is 306 MPa, which occurs at the rectangular corner of the supporting rails. And the maximum equivalent stress of jacket and CuCrZr conductor are 170 MPa and 38 MPa respectively. The peak stresses are located near the middle region of the components. Since the regions bear higher nuclear radiation than that at the two ends.

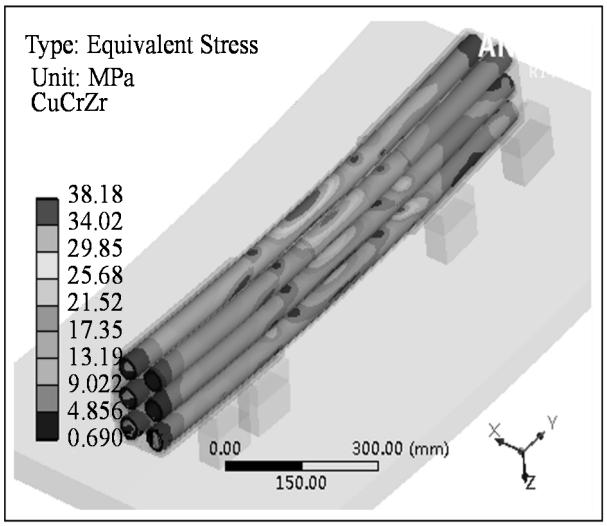

Fig. 9 *The equivalent stress on CuCrZr conductor*

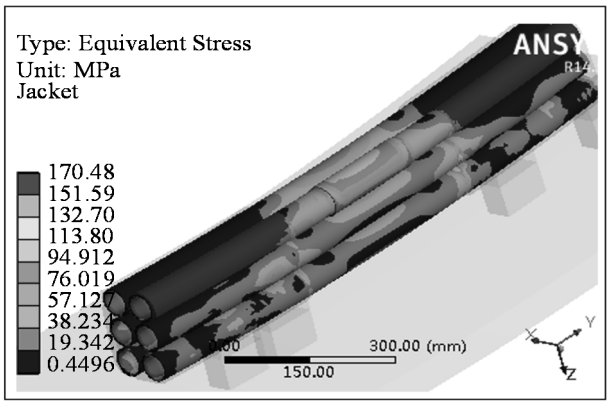

Fig. 10 *The equivalent stress on jacket*

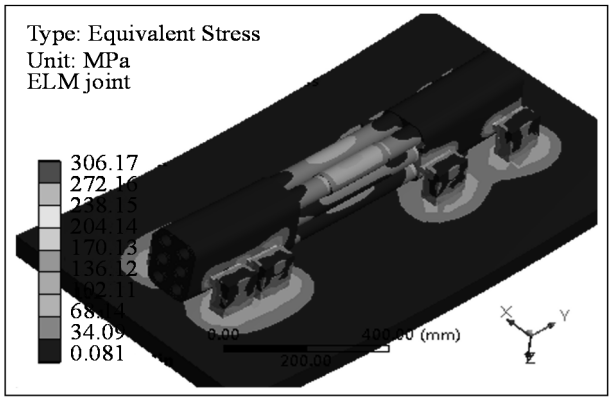

Fig. 11 *The equivalent stress on ELM joint*

3.2 The structural optimization of supporting rail

The above mechanical analyses show that stress intensity occurs at the corner of the supporting rails. In order to mitigate stress intensity, the fillets with different radii are tested for the corner. If the radius of fillet is set as 5 mm, the maximum stress will fall down from 306 MPa to 275 MPa. If the fillet radius is increased to 10 mm, the maximum stress will decrease to 227 MPa. The detailed equivalent stress on the supporting rail are presented in Fig. 12. Furthermore, if we set the fillet radius as 12 mm, the maximum stress will decrease to 213 MPa. To more conveniently compare the stress variation under different fillet radius, the different kinds of stress are extracted and listed in table 1. It indicates that increasing fillet radius is an effective solution to decrease stress intensity.

Tab. 1 *Equivalent stress of supporting rail under different fillet radius*

Stress (MPa)	R= 0	R= 5 mm	R= 10 mm	R=12 mm	Threshold
P_m	210	161.7	159.2	143.6	191
P_L+P_b	275	185.4	193.3	201.7	286.5
Q	306	275	227	213	573

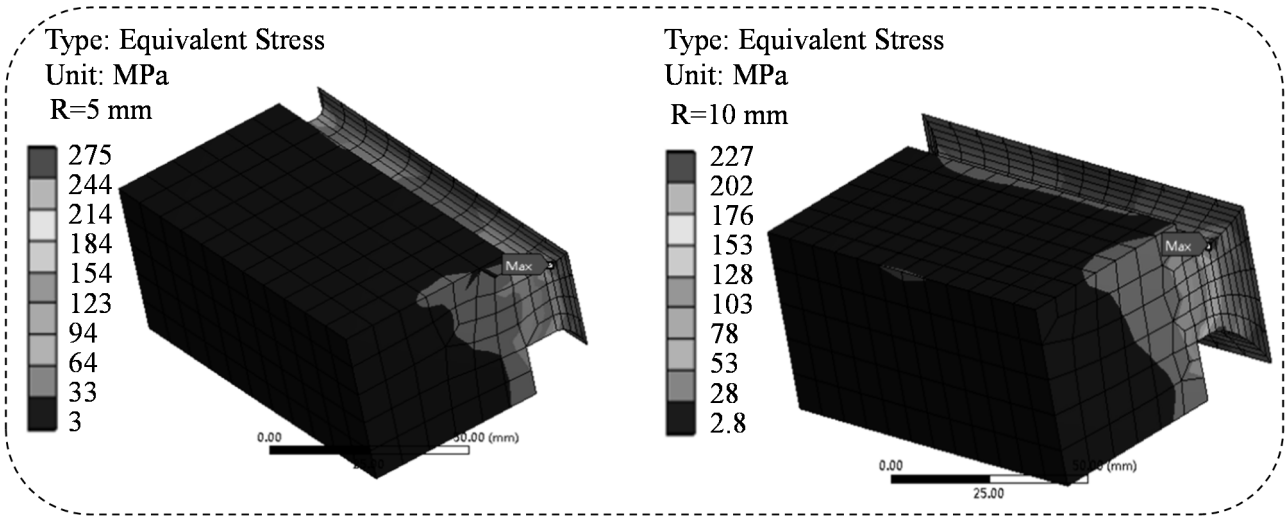

Fig. 12 *The equivalent stress on supporting rail with different fillet radius*

4 Stress evaluation for ELM joint

Two different methods are usually used for stress evaluation, namely the routine design and analytical design. The routine design is based on the first strength theory. The evaluation criterion is a little conservative for pressure vessel and tube components. Here analytical design is selected, which is based on the fourth strength theory. For analytical design, the stresses are classified and accessed with different thresholds [14]. According to types of the external load inducing inner stress, the stresses are classified into general membrane stress, local membrane stress, bending stress, peak stress and secondary stress. The general membrane stress should be within the design stress intensity Sm. The local membrane stress plus bending stress are not allowed beyond 1.5 S_m. The secondary stress is not allowed beyond 3.0 S_m. Here the design stress intensity is determined by the material yield strength and ultimate strength. And it equals to the lesser magnitude of 2/3 yield strength and 1/2 ultimate strength. For ELM joint, it needs to bear the external loads such as dead weight, thermal load and electromagnetic force. Since the stress induced by dead weight is tiny, it is ignored in the mechanical analysis. The electromagnetic load as volumetric force will generate membrane plus bending stress. And the corresponding threshold is 1.5 S_m. The Joule heat and nuclear heat as thermal load will induce secondary thermal stress. And the corresponding threshold is 3.0 S_m. Note that the design stress intensity is related with temperature. The thresholds of joint materials under 100℃ and 200℃ are presented in Table 2. Considering the temperature rising of ELM joint, the thresholds at 200℃ are used for stress evaluation. The different kinds of stress are extracted through the method of stress linearization. The maximum secondary stress occurs on the CuCrZr conductor is 38 MPa, which is far less than the threshold of 435 MPa. The maximum secondary stress of the supporting rail is 306 MPa, which is within the threshold of 537 MPa. While the maximum general membrane stress on supporting rail without fillet is 210 MPa, which is beyond the threshold of 191 MPa. Once the 12 mm-radius fillet is added, the maximum general membrane stress falls down to 144 MPa. There is sufficient safety margin. Thus, it is necessary and feasible to add fillets on supporting rail to decrease the stress.

Tab. 2 *The stress evaluation criterion*

Stress type	Stress limit (MPa)			
	CuCrZr		Inconel 625	
	100℃	200℃	100℃	200℃
P_m	153	145	218	191
P_L+P_b	229.5	217.5	327	286.5
Q	459	435	654	573

5 Conclusion

To verify the mechanical performance of ELM joint under multi-load cases, the electromagnetic analysis is launched first. The analysis indicates the equatorial joint bears the highest magnetic field of 4.84 T. Thus, it is selected as the representative joint for the mechanical analysis. The heat deposition induced by Joule heat and nuclear radiation is calculated subsequently. And the peak Joule heat and nuclear heat densities are 2.95 and 1.12 $MW \cdot m^{-3}$ respectively. Then the temperature is calculated by imposing the Joule heat and nuclear heat into the thermal analysis model.

The analysis results show that the highest temperature occurs at supporting rail with the value of 263 ℃. After the electromagnetic and thermal analyses, the electromagnetic force density and temperature and employed as boundary condition to carry out mechanical analysis. The analysis results show that stress intensity occurs at supporting rail. While after adding fillets on supporting rail, the maximum equivalent stress will be decreased significantly. Finally, the different kinds of stress on ELM joint is extracted through stress linearization. And the stress is assessed based on analytical design. It demonstrates that the general membrane stress on the supporting rail will be controlled within the threshold after adding fillet.

Acknowledgement

This project has been financially supported by the Talent Project of Jiangsu Institute of Technology (Grant No. KYY16002) and the Project of Background Field Magnets (Grant No. KYH20148).

References

[1] FITZPATRICK, RICHARD. (2020). Theory of edge localized mode suppression by static resonant magnetic perturbations in the DIII-D tokamak. In: *Physics of Plasmas*, Vol. 27, No. 4, Art. No.: 042506. AMER. USA.

[2] TANG T.F., XU X.Q., LI, G.Q., et al. (2021). Edge-localized-mode simulation in CFETR steady-state scenario. In: *Nuclear Fusion*, Vol. 62, No. 1, Art. No.: 016008. IOP. England.

[3] KLEINER A., FERRARO N.M., DIALLO A., et al. (2021). Importance of resistivity on edge-localized mode onset in spherical tokamaks. In: *Nuclear Fusion,* Vol. 61, No. 6, Art. No.: 064002. IOP. England.

[4] SHI YI, WU YU, JIN HUAN, et al. (2014). The experiment progress of bracket brazing to SSMIC for the ITER ELM prototype coil. In: *Fusion engineering and design*, Vol. 89, No. 11, pp. 2776-2783. ELSEVIER. Netherlands.

[5] FENG LONG, YU WU, HUAN, JIN, et al. (2014). R&D activities on ITER In-Vessel Coil SSMI conductor fabrication. In: *IEEE Transactions on Applied Superconductivity*, Vol. 24, No. 3, Art. No.: 6646234. IEEE. USA.

[6] G. KALININ, V. BARABASH, A. CARDELLA, et al. (2000). Assessment and selection of materials for ITER in-vessel components. In: *Journal of Nuclear Materials*, Vol. 283, pp. 10-19. Elsevier. Netherlands.

[7] H. JIN, Y. WU, F. LONG, et al. (2013). Investigation and analysis on ITER In-Vessel coils' raw-materials. In: *Fusion Engineering and Design*, Vol. 88, No. 11, pp. 3028–3032. Elsevier. Netherlands.

[8] XIANEWEI WANG, PENG HAN, QING HE, et al (2019). Induction Brazing Analysis of EAST Fast Control Coil Conductor. In: *Manufacturing Technology,* Vol. 19, No. 5, pp. 896-902. Engineering Village. USA.

[9] ZHANG SW, SONG YT, WANG ZW, et al. (2014). Mechanical Analysis and Optimization of ITER Upper ELM Coil & Feeder. In: *Plasma Science and Technology*. Vol. 16, No. 8, pp. 794-799. IOP. England.

[10] XIANEWEI WANG, PENG HAN, QING HE, et al. (2020). The Thermal and Structural Analysis of Vertical Stability Coil. In: *Manufacturing Technology*, Vol. 20, No. 1, pp. 120-125. Engineering Village. USA.

[11] CHEN ZHAOXI, VULLIEZ KARL, FERLAY FABIEN, et al. (2015). Design and optimization of the WEST ICRH antenna front face components based on thermal and hydraulic analysis. In: *Fusion Engineering and Design*, Vol. 94, pp. 82-89. Elsevier. Netherlands.

[12] LIU LIMIN, ZHANG DALIN, LU QING, et al. (2016). Preliminary neutronic and thermal-hydraulic analysis of a 2 MW Thorium-Based Molten Salt Reactor with Solid Fuel. In: *Progress in Nuclear Energy*, Vol. 86, pp. 1-10. Pergamon-Elsevier Science LTD. England.

[13] SONTAMINO, ARKARAPON, PHANITWONG, et al. (2017). Finite element analysis of counterbore shaped parts by using sheet-bulk metal forming process. In: *Manufacturing Technology*, Vol. 17, No. 4, pp. 597-602. Engineering Village. USA.

[14] Boiler and pressure vessel committee (2001). *Boiler and pressure vessel code*, Section III, NB-3000, American Society of Mechanical Engineers.